JOURNAL OF NANO- AND ELECTRONIC PHYSICS
Vol. **18** No 5, 05002(7pp) (2026)

ЖУРНАЛ НАНО- ТА ЕЛЕКТРОННОЇ ФІЗИКИ
Том **18** № 5, 05002(7cc) (2026)

OPEN ACCESS

REGULAR ARTICLE

Implementation of Novel 3D Printed Perturb Microwave Laminate with Circular Mesh Grid Substrate for Circularly Polarized Patch Antenna

Monalisa Pal[1,2], Soumendra Pain[1,2,3], Umesh Shrikrishna Patkar[1,2], Tapas Mondal[3,*]

[1] *Intelligent Systems Engineering Group, CSIR-Central Mechanical Engineering Research Institute, 713209 Durgapur, West Bengal, India*
[2] *Academy of Scientific and Innovative Research (AcSIR), 201002 Ghaziabad, UP, India*
[3] *Electronics and Communication Engineering Department, Dr. B. C. Roy Engineering College, 713206 Durgapur, West Bengal, India*

(Received 18 April 2026; revised manuscript received 23 October 2026; published online 28 October 2026)

This paper presents the design and implementation of a novel 3D printed microwave laminate consisting of identical circular slots in mesh grid fashion to incorporate the volume fraction of air influencing the effective permittivity and as a result suitable for antenna fabrication. Along with identical circular slots, four perturbations are introduced with rectangular shaped polymer partially filling them. This type of asymmetric structure in the substrate layer that leads to the splitting of the degenerate modes of the planar antenna, thus emitting circularly polarized electromagnetic waves. This dielectric substrate was manufactured by 3D printing using an opaque, impact-resistant engineering thermoplastic and both sides coated with thin copper layer. The proposed antenna was implemented with double stack substrate layer to accommodate the hat shaped feeding structure as well as ground in the bottom and circular radiating patch in the top layer which exhibits axial ratio beamwidth of 177°. Consumer Wi-Fi hotspots & smart home systems, intelligent transport systems and roadside units, and GPS tracking are probable application areas of the proposed low- profile antenna.

Keywords: Microwave laminate, 3D printed material, Circularly polarized antenna, Circular patch antenna.

DOI: 10.21272/jnep.18(5).05002 PACS number: 84.40.Ba

1. INTRODUCTION

The use of layered manufacturing technology, commonly known as 3-dimensional printing or rapid prototyping, in the design process of antennas has risen tremendously due to the numerous benefits associated with the process. Some of these benefits include flexibility in manufacturing processes, fast production rates, and lower costs as compared to the traditional approaches used in manufacturing prototypes. First, additive manufacturing allows the engineers and researchers to manufacture prototypes very easily, unlike using traditional methods of manufacturing, such as etching and machining. This saves on the time that would have been required to make the antenna. Secondly, 3D printing offers the benefit of manufacturing complex geometries, some of which cannot be made using conventional manufacturing methods. Such geometries include conformal antennas, antennas embedded in structures, and substrates composed of dielectric gradients. Thirdly, another benefit of using additive manufacturing in designing antennas is that it allows for the fabrication of lightweight structures because most printing materials are usually polymer-based. This makes antennas produced using additive manufacturing technology ideal for aerospace, UAVs, and wearable devices. Lastly, additive manufacturing offers the unique capability of controlling dielectric properties.

Some popularly used 3D printing materials are Acrylonitrile Butadiene Styrene (ABS), Polylactic acid (PLA) etc. Among these materials Acrylonitrile Butadiene Styrene (ABS) is preferred for 3D printed antenna substrate for its optimum mechanical and electrical properties. ABS has dielectric constant of about 2.7 which is suitable for antennas designed for low to medium frequency applications such as the 2.4 GHz ISM band and a loss tangent ($\tan\delta$) of 0.005, which is higher compared to specialized RF materials, acceptable for prototyping purposes. Moreover, ABS shows excellent electrical insulation, toughness and impact resistance to cracking or deformation during handling and operation as compared to PLA which is brittle, less durable and has lower heat resistance as it has lower glass transition temperature of 55-65°C, so it begins to deform at relatively moderate temperatures. ABS has a higher glass transition temperature (T_g) of around 105 °C, which means it can withstand higher temperatures before it starts to soften and lose its shape thus showing higher thermal stability, durability and reliability. ABS is scratch resistant and can withstand temperatures ranging from + 70 to – 50°C [1-5]. Various properties like thermal and dimensional stability, high-impact strength, and chemical resistance make ABS particularly suitable for antennas that need to function in moderately demanding environments. The paper [12]

* Correspondence e-mail: tapas2k@gmail.com

© 2026 The Author(s). Journal of Nano- and Electronic Physics published by Sumy State University. This article is distributed under the terms and conditions of the Creative Commons Attribution (CC BY) license.

Cite this article as: M. Pal et al., *J. Nano- Electron. Phys.* 18 No 5, 05002 (2026) https://doi.org/10.21272/jnep.18(5).05002

proposes a 3D-printed frequency-reconfigurable circularly polarized microstrip antenna with reduced parasitic and wide tuning capability using vertically integrated varactor-loaded L-slot design. A wideband circularly polarized stacked patch antenna with broad beamwidth is proposed [13] using a rectangular shell beneath the ground structure. The antenna achieves over 140° 3 dB beamwidth, 10.2 % CP bandwidth, and 52. 8% impedance bandwidth at 2.4 GHz, making it suitable for wide-angle scanning phased array applications.

The proposed work introduces a novel circularly polaised coaxial fed antenna comprising of 3D printed substrate with circular cells in grid pattern and circular shaped patch. The antenna has high gain and a wide transmission bandwidth. The Fused Deposition Modelling (FDM) technology, also known as Fused Filament Fabrication (FFF) technology has been used for additively manufacturing the two substrate layers using thermoplastic material – acrylonitrile butadiene styrene (ABS) [6-10]. The substrate for the proposed antenna consists of a dual layer circular grid made up of both thermoplastic and air. The first reason for this is that the introduction of two pieces of thermoplastic in the substrate causes an imbalance that helps create circularly polarised (CP) waves. The second reason is that it is possible to change the proportion of air volume within the substrate, which alters the permittivity of the substrate and consequently the 3 dB axial ratio beamwidth. The success of the proposed technique is supported by fabricating a model whose results show high correlation with simulation results.

2. PROPOSED ANTENNA GEOMETRY

Fig. 1 illustrates the disassembled view of the proposed coaxial-fed CP patch antenna. Although both substrates and ground have square shapes with dimensions of $l = 12$ cm on all sides, the patch, however, has a circular shape with radius $r = 2.3$ cm. In order to match impedance to the coaxial feeding system with an impedance of 50 Ω, a square shaped top hat of 1 cm is placed under the patch with respect to the diagonal line, and it occupies two substrate layers. The side dimension of the top hat is denoted as b. On the other hand, h_1 and h_2 are the dimensions of the top and bottom layers of the substrate, respectively. The perturbation layer that occurs in the lower layer takes the shape of a semicircle. Radius of the repetitive circular cells in the both substrate is represented by r_s and the radius is 0.4 cm. Fig. 2 and Fig. 3 represent the detailed views of the bottom layer and top layer of the additively fabricated substrate, respectively. In order to simplify the installation process, both substrate layers are glued together through industrial grade glue. Table 1 presents the dimensions of the proposed antenna.

The inner region consists of a circular mesh grid arrangement having a fixed radius of $r = 0.4$ cm for each cell which is filled with air, except for two sets of cells that are proportionally arranged on the central line in the x-direction. Two thermoplastic material pieces partially occupy the special cells, which are located in the xy-plane at a separation of d from the adjacent polymer wall. Moreover, the dimensions of W_x and W_y represent the distance between two adjacent air-filled slots in the x and y-directions, consecutively.

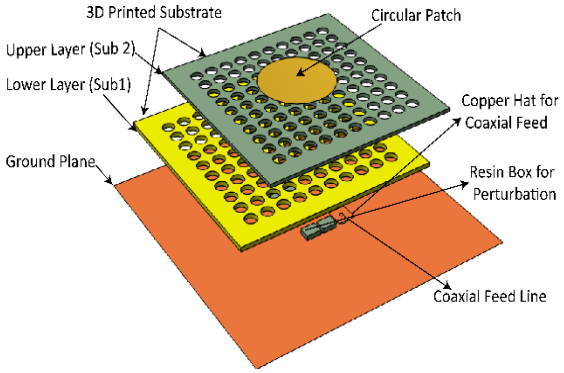


Fig. 1 – The dis-assembled view of the proposed circular mesh CP antenna with two layers of substrate

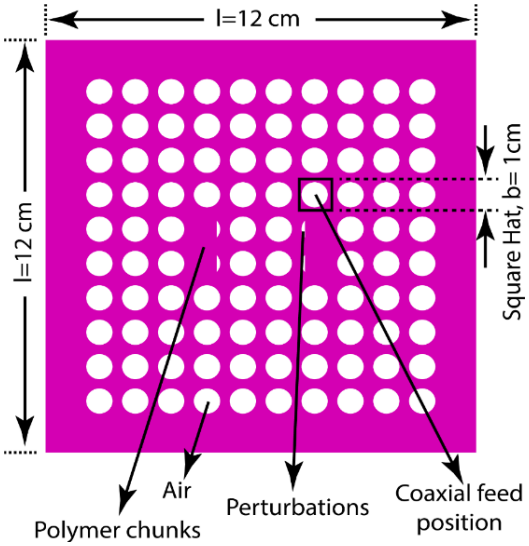


Fig. 2 – Detailed view of the bottom layer of air-filled 3D printed ABS substrate

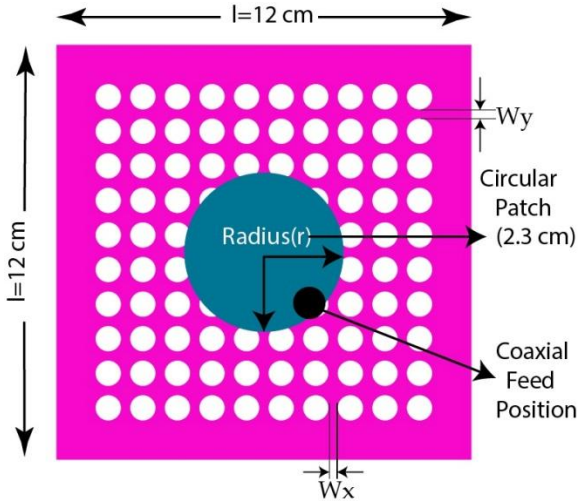


Fig. 3 – Detailed view of the top layer of 3D printed ABS substrate with circular patch

Table 1 – Design specifications of the proposed antenna

Specifications	r	h_1	l	h_2
Values in cm	2.3	0.2	12	0.25
Specifications	W_x	W_y	b	r_s
Values in cm	0.26	0.26	1	0.4

3. 3D PRINTING OF SUBSTRATE

The double layer substrate of the proposed antenna has been 3D printed using Acrylonitrile Butadiene Styrene (ABS) material which needed the following settings for the 3D printer at the time of printing. The 3D printing of two layers of substrate was completed in approximately five hours. Fig. 4 (a) and Fig. 4 (b) illustrates the interface of slicing software UltiMaker Cura™.

Table 2 – Settings for the 3D printer for the Acrylonitrile Butadiene Styrene (ABS) material as substrate

Settings	Values
Nozzle Temperature	230 °C±2
Bed Temperature	100 °C±2
Infill Density	10 %
Layer Height	0.15mm
Wall Line Count	3
Top Layers	6
Bottom Layers	4
Cooling During Printing	0 %
Build Plate Adhesion	Brim
Support	No support was required

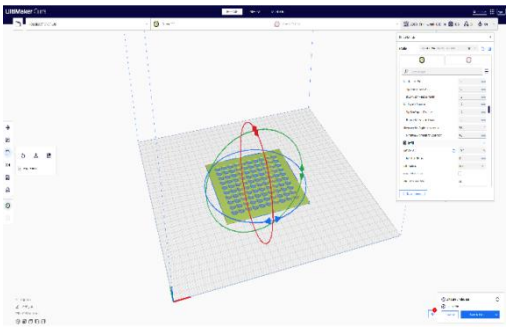


Fig. 4 – (a) Top Layer

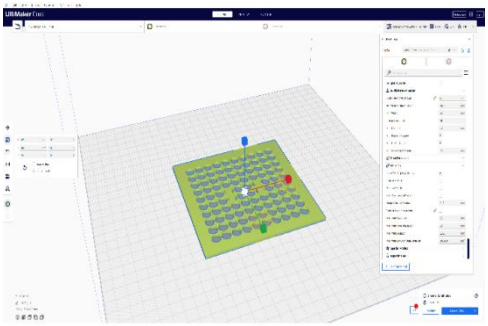


Fig. 4 – (b) Bottom Layer

Fig. 4 illustrates the interface of the slicing software showing the printing time required for (a) upper substrate layer to be 2 hours and that of the (b) lower layer with thermoplastic polymer blocks to be 2 hours 32 minutes.

4. OPERATING PRINCIPLE OF THE ANTENNA

4.1 Generation of CP

While the process of linear polarization requires strict oscillations in one plane, the CP method requires that the electromagnetic wave's electric field vector should rotate in a circular manner. To convert linear polarization to circular polarization, the CP antenna does not need any further components. This is because it might be necessary to have an extra component in linear polarization antennas to enable the conversion of the broadcast or reception of a linear signal into circu-

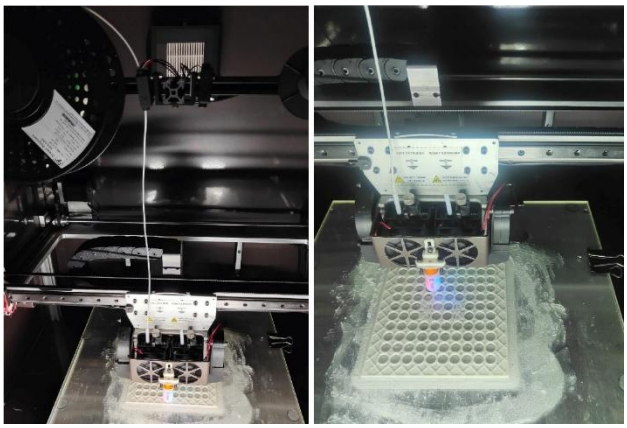
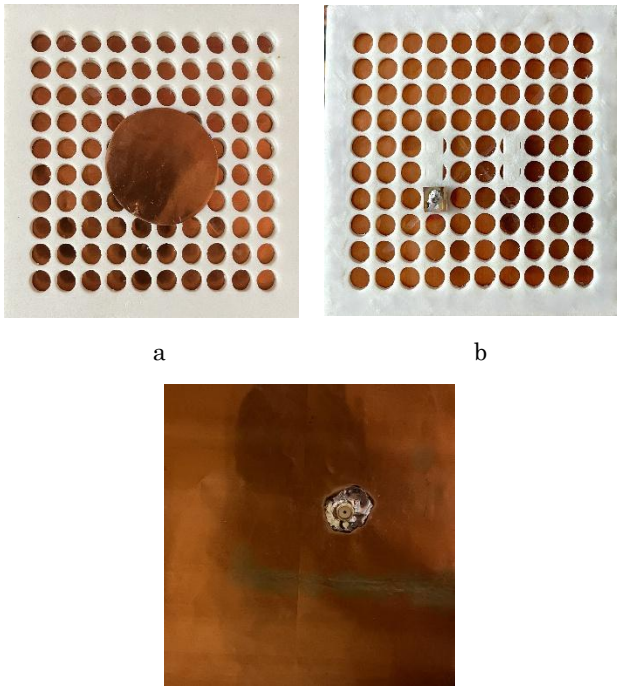


Fig. 5 – The photograph illustrates the 3D printing process of one of the layers of substrate



a b c d

Fig. 6 – (a) 3D printed top layer (b) 3D top layer of bottom substrate (c) ground of antenna with coaxial feed (d) side view of additively manufactured prototype of CP patch antenna

lar form. This means that single-fed CP antennas can be designed in a manner that enables the emission of circular polarization waves.

$$f_x = c/[2W_x\sqrt{e_{rx}}] \quad (1)$$

$$f_y = c/[2W_y\sqrt{e_{ry}}] \quad (2)$$

Taking this feature into account, the single feed CP antennas would be simpler and more efficient due to their lack of need for additional components, which may reduce costs, complexity, and even potential problems with the design. Moreover, they can simplify the process of implementation in the case when circular polarization must be generated. The presented CP antennas operate based on the basic concept of forming a circular patch with an aim to achieve non-uniform effective lengths of two orthogonal sides. An alternate technique is adopted for generating CP radiation in this paper, as depicted in Fig. 2, where the substrate beneath the patch is fabricated using varying effective dielectric constant in various directions. The two ABS materials have been presented, where they have longer sides in the y-direction compared to the x-direction. This leads to somewhat reduced relative dielectric constant, which is ϵ_{rx} and ϵ_{ry}.

Thus, according to Eqs. (1) and (2), it is possible to separate the two degenerate modes in some way, showing that the impact of the perturbation on shape is similar to the impact of the difference in the effective permittivity. In another case, the substrate provides the required alteration for CP instead of the patch. Fig. 7 shows the surface current distribution of the circular patch within the period T, where $t = T/4$ at frequency 2.4 GHz. It is observed that LHCP of the CP patch antenna is achieved.

4.2 Beamwidth Generation

This CP patch antenna can be conceptualized as an array of two pairs of parallel magnetic currents in a circular shape, in accordance with the traditional patch antenna theory [11-14]. Consequently, we can express the orthogonal, normalized far-field electric field components, E_θ and E_ϕ within the xz and yz planes as follows:

$$E_\theta = \cos(\pi \frac{\sin(\theta)Wpe}{\lambda}) \quad (3)$$

$$E_\phi = \frac{\sin(\pi\frac{\sin(\theta)Wpe}{\lambda})}{\pi\frac{\sin(\theta)Wpe}{\lambda}}\cos(\theta) \quad (4)$$

Here, W_{pe} is the width of effective patch and λ is the wavelength of free-space. Assuming that the quadrature phase is observed in E_θ and E_ϕ, Axial Ratio is obtained as

$$\text{Axial Ratio} = \left|20log_{10}\left(E_\theta/E_\phi\right)\right| \quad (5)$$

From (2) and (3) we find that AR depends on W_{pe}/λ. Furthermore,

$$W_{pe} = \lambda/2\,\text{sqrt}(\varepsilon_{reff}) \quad (6)$$

and

$$\varepsilon_{reff} = [\varepsilon_r + 1]/2 + [\varepsilon_r - 1] * \left[1 + 12h/W_p\right]^{-1/2}/2 \quad (7)$$

represent the circular patch antenna electrical width functioning in the dominant TM_{01} mode. Here, ε_r denotes the relative permittivity of the substrate, and ε_{reff} the effective relative permittivity of the resulting patch antenna. ε_r, h, and W_p are the factors on which W_{pe}/λ depends, in accordance with Eqs. (4) and (5). The relative permittivity of the substrate is the only factor that may define the 3 dB axial ratio beamwidth of the resulting circular patch antenna, which has a constant height and side length.

To meet realistic design requirements for the substrate's relative permittivity, a circular mesh-grid structure was 3D-printed, as illustrated in Fig. 2. This substrate features air-filled cells with walls constructed from Acrylonitrile Butadiene Styrene (ABS), which has a relative permittivity of 2.7. Thus, the substrate's overall permittivity can be tuned by changing the ratio of the two different materials. Effective relative permittivity of the entire substrate may be calculated using the Landau and Landau-Lifshitz-Looyenga [7].

$$(\in_r)^{\frac{1}{3}} = v_1(\in_{r1})^{\frac{1}{3}} + v_2(\in_{r2})^{\frac{1}{3}} \quad (8)$$

where v_1 and v_2 denote the volume fractions of the respective constituent materials, represented by $w/(w + w_s)$ and $w_s/(w + w_s)$, whereas $\in_{r1}$ and $\in_{r2}$ represent relative permittivity of thermoplastic polymer and air, respectively. Moreover, effective permittivity is calculated and formulated through the Nielsen-Ross-Weir approach, aided by ANSYS HFSS™. The 3 dB axial ratio beamwidth (ARBW) of the proposed patch antenna with dissimilar values of w_s along with the calculated and simulated values of relative permittivity ε_r of the air-filled substrate are provided in Fig. 7. A good level of agreement exists among all the computed and simulated results. Thus, it is possible to correctly manage not only the substrate's permittivity but also the 3dB ARBW of the suggested antenna.

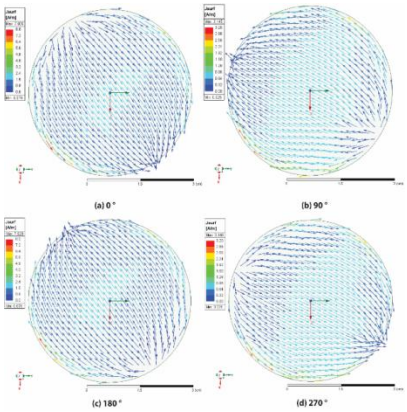


Fig. 7 – Surface current distribution across four phase intervals on the circular patch at 2.4 GHz (a) 0°, (b) 90°, (c) 180° (d) 270°

5. PARAMETRIC STUDY OF THE ANTENNA

It was found that replacing the substrate material with FR4 leads to a reduction in antenna gain from 7.15 dBi to 4.81 dBi. Fig. 8 and Fig. 9 presents a comparison of the simulated reflection coefficients results of the fabricated CP antenna prototype under two different conditions: **(i)** when comparing the antenna with

a dual-layer ABS substrate against one with a dual-layer FR4 substrate; **(ii)** with and without circular gaps in the both layers of the substrate.

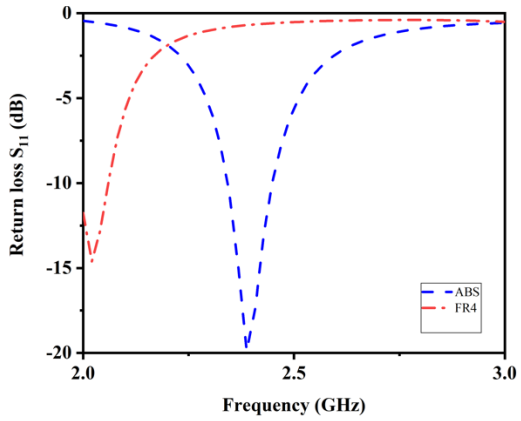


Fig. 8 – The graph compares the simulated reflection coefficients for two versions of the fabricated CP antenna prototype: one using ABS for both substrate layers, and the other using FR4

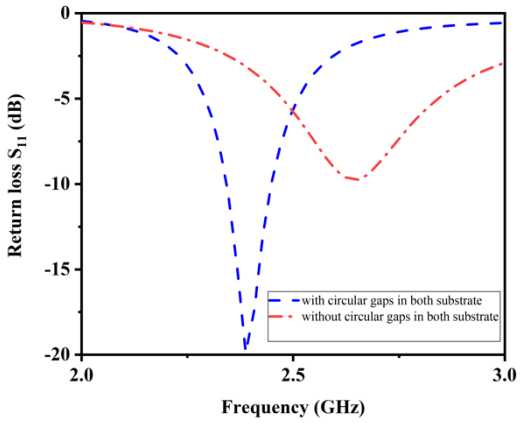


Fig. 9 – The graph illustrates the comparative study of simulated results of reflection coefficients of CP antenna prototype with and without circular gaps in the substrate material

The incorporation of a circular shaped mesh structure within the substrates produced improved performance in terms of reflection coefficient, compared to substrates without circular shaped structures. Furthermore, a comparison of simulated and measured reflection coefficients was carried out for designs with FR4 as a substrate material and ABS as a substrate material.

6. FABRICATION AND EXPERIMENTAL RESULTS

Fig. 5 presents the 3D printing setup, the printing process of one of the substrates and the Fig. 6 shows the fabricated antenna prototype with its circular mesh substrate respectively. The antenna structure consists of the ground plane, 3D-printed substrate, and circular shaped patch, assembled and firmly bonded using industrial grade adhesive. The top hat is accurately fitted into the substrate, confirming the mechanical stability of the design. Fig. 10 shows the comparison between measured and simulated axial ratio (AR) of the proposed antenna. Minimum AR values of 1.39 dB at 2.44 GHz (measured) and 0.84 dB at 2.436 GHz (simulated) are obtained, with bandwidths of 3.4 % and 3.5 %, respectively. The reflection coefficients in Fig. 11 show close agreement between measurement and simulation, with 10 dB impedance bandwidths of 2.3533-2.4600 GHz (measured) and 2.3450-2.4525 GHz (simulated). Three-dimensional radiation pattern with the antenna prototype is illustrated in Fig. 12. 3 dB AR beamwidth of 178° is achieved, indicating suitability for wide-beam applications. Table 3 compares our design with previous work in the literature. This comparison clearly highlights that our proposed antenna achieves a much simpler and lower-profile design, along with moderately high gain, wide axial ratio bandwidth, and broad 3 dB axial ratio beamwidth.

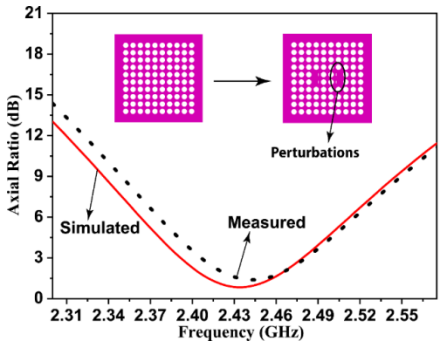


Fig. 10 – Simulated versus measured axial ratio for the CP antenna prototype

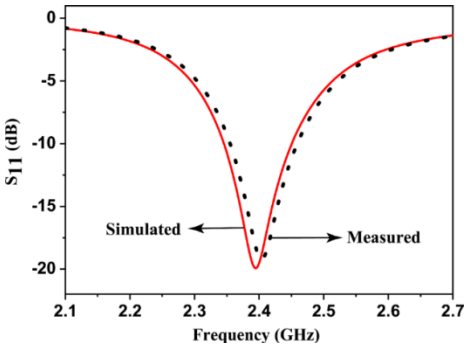


Fig. 11 – A comparison of the predicted and experimentally tested reflection coefficients S_{11} of the prototype antenna

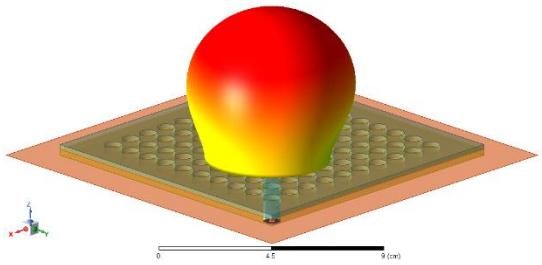


Fig. 12 – Three-dimensional radiation pattern of the proposed CP antenna prototype

Table 3 – Comparison between previous works and our work

References	[12]	[13]	Proposed Work
Feed	Single	Single	Single
AR Bandwidth	3 %	10.2 %	3.7 %
Gain (dBi)	4.5	3.7	7.15
Height (λ_0)	0.006	–	0.45
3dB ARBW	–	1750	1770

7. CONCLUSION

This paper introduces a new coaxially-fed, circularly polarized (CP) circular patch antenna designed for 2.4 GHz operation, utilizing an inherently asymmetric circular shaped mesh-grid substrate. The design achieves a high gain of 7.15 dBi. Asymmetry required for CP radiation is introduced through four distinct unit cells arranged along a central axis, resulting in left-hand circular polarization (LHCP) with an axial ratio bandwidth of 90 MHz (2.390-2.480 GHz). The substrate is fabricated using fused deposition modelling (FDM) 3D printing, enabling a compact, low-profile structure. The antenna also exhibits a 10 dB impedance bandwidth of 107.5 MHz (2.3450-2.4525 GHz), making it suitable for applications like IoT devices, smart home systems, intelligent transportation and roadside units, and GPS tracking.

ACKNOWLEDGEMENTS

The proposed antenna was successfully fabricated at the state-of-the-art laboratory facility at Dr. B. C. Roy Engineering College, Durgapur. This work was carried out under the Finishing School Program on 3D Printing and Additive Manufacturing Technology, implemented by the Centre for Development of Advanced Computing (C-DAC) with funding support from the Ministry of Electronics and Information Technology (MeitY), Government of India (Administrative Approval No. L-14011/6/2024-HRD) and Intelligent System Engineering Laboratory, CSIR-Central Mechanical Engineering Research Institute, Durgapur – 713209, West Bengal, India.

DECLARATION OF COMPETING INTEREST

The authors declare no competing financial interests or personal relationships that could have influenced the work presented in this paper.

DATA AVAILABILITY

Data will be made available on request.

AUTHORSHIP CONTRIBUTION STATEMENT

Monalisa Pal: Writing – Review & editing, Writing – original draft, Methodology, Investigation, Formal analysis; **Soumendra Pain:** Writing – review & editing, Writing– original draft, Methodology, Investigation; **Umesh Shrikrishna Patkar:** Investigation, Formal analysis, Supervision, Conceptualization, Project administration; **Tapas Mondal:** Investigation, Formal analysis, Supervision, Conceptualization, Project administration.

REFERENCES

1. Oadby Plastics Ltd, "ABS Technical Datasheet," 2025. [Online]. Available: ABS Technical Datasheet.
2. C. Abeykoon, P. Sri-Amphorn, A. Fernando, *International Journal of Lightweight Materials and Manufacture* **3** No 3, 284 (2020) https://doi.org/10.1016/j.ijlmm.2020.03.003.
3. M. Samykano, S.K. Selvamani, K. Kadirgama, et al., *International Journal of Advanced Manufacturing Technology* **102**, 2779 (2019) https://doi.org/10.1007/s00170-019-03313-0.
4. B.S. Dhaliwal, K. Singla, G. Saini, *IEEE Indian Conference on Antennas and Propagation* (InCAP), 984 (2021) https://doi.org/10.1109/InCAP52216.2021.9726492.
5. N.W. Liu, L. Zhu, W.-W. Choi, *IET Microwaves, Antennas & Propagation* **10** No 8, 885 (2016) https://doi.org/10.1049/iet-map.2016.0081.
6. G. Muntoni, *IEEE Open Journal of Antennas and Propagation* **3**, 1351 (2022) https://doi.org/10.1109/OJAP.2022.3222454.
7. M. Ramadan, R. Dahle, *IEEE Transactions on Antennas and Propagation* **67**, 2896 (2019) https://doi.org/10.1109/TAP.2019.2896762.
8. P. Njogu, B. Sanz-Izquierdo, A. Elibiary, S.Y. Jun, Z. Chen, D. Bird, *IEEE Access* **8**, 228711 (2020) https://doi.org/10.1109/ACCESS.2020.3043045.
9. M. Liang, C. Shemelya, E. MacDonald, R. Wicker, H. Xin, *IEEE Antennas and Wireless Propagation Letters* **14**, 1346 (2015) https://doi.org/10.1109/LAWP.2015.2405054.
10. D.R. Jackson, *Microstrip antennas, Ch. 7* in *Antenna Engineering Handbook* (New York, NY, USA: McGraw-Hill: 2007).
11. C.A. Balanis, *Antenna Theory: Analysis and Design* (Hoboken, NJ, USA: Wiley: 2005).
12. M.F. Farooqui, A. Kishk, *IEEE Antennas and Wireless Propagation Letters* **18**, 1429 (2019) https://doi.org/10.1109/LAWP.2019.2919255.
13. Z. Xue, W. Li, W. Ren, H. Jiang, *Electronics Letters* **51**, 10 (2015) https://doi.org/10.1049/el.2014.3783.
14. S.S. Carvalho, J.R.V. Reis, A. Mateus, R.F.S. Caldeirinha, *IEEE Access* **12**, 10718 (2024) https://doi.org/10.1109/ACCESS.2024.3354372.

Реалізація інноваційного мікрохвильового ламінату, виготовленого методом 3D-друку, із підкладкою у вигляді кругової сітчастої структури для мікросмужкової антени з круговою поляризацією

Monalisa Pal[1,2], Soumendra Pain[1,2,3], Umesh Shrikrishna Patkar[1,2], Tapas Mondal[3]

[1] *Intelligent Systems Engineering Group, CSIR-Central Mechanical Engineering Research Institute, 713209 Durgapur, West Bengal, India*
[2] *Academy of Scientific and Innovative Research (AcSIR), 201002 Ghaziabad, UP, India*
[3] *Electronics and Communication Engineering Department, Dr. B. C. Roy Engineering College, 713206 Durgapur, West Bengal, India*

У статті представлено проєкт і реалізацію нового мікрохвильового ламінату, виготовленого методом 3D-друку. Він містить ідентичні круглі отвори, розташовані у вигляді сітки, що дозволяє регулювати об'ємну частку повітря, яка впливає на ефективну діелектричну проникність, роблячи такий матеріал придатним для створення антен. Окрім круглих отворів, у структуру введено чотири елементи з полімеру прямокутної форми, які частково заповнюють ці отвори. Така асиметрична будова підкладки призводить до розщеплення вироджених мод планарної антени, завдяки чому вона випромінює електромагнітні хвилі з круговою поляризацією. Діелектричну підкладку було виготовлено за допомогою 3D-друку з використанням непрозорого ударостійкого інженерного термопласту; обидві її сторони вкриті тонким шаром міді. Запропонована антена має двошарову підкладку, що дозволяє розмістити в ній живильну структуру «капелюшного» типу, а також заземлювальний шар (знизу) та круглий випромінювальний елемент (зверху). Така конструкція забезпечує ширину діаграми спрямованості за осьовим відношенням у 177°. Серед можливих сфер застосування цієї низькопрофільної антени – побутові точки доступу Wi-Fi та системи «розумного дому», інтелектуальні транспортні системи й придорожнє обладнання, а також системи GPS-відстеження.

Ключові слова: Мікрохвильовий ламінат, Матеріал, виготовлений методом 3D-друку, Антена з круговою поляризацією, Кругла мікросмужкова антена.